Available online at www.sciencedirect.com

SCIENCE DIRECT®

Cold Regions Science and Technology 39 (2004) 161–180

cold regions science and technology

www.elsevier.com/locate/coldregions

# Computing extreme avalanches

Christophe Ancey*, Christian Gervasoni, Maurice Meunier

*École Polytechnique Fédérale de Lausanne, Laboratoire d'Hydraulique Environnementale, Ecublens, 1015 Lausanne, Switzerland*
*Politecnico di Milano, Hydraulics Division, Piazza Leonardo da Vinci, 32, 20133 Milan, Italy*
*Cemagref, Unité Erosion Torrentielle, Neige et Avalanches, Domaine Universitaire, 38402 Saint-Martin-d'Hères Cedex, France*

Accepted 26 April 2004

**Abstract**

Increasing the reliability and accuracy of avalanche zoning method is of primary importance in heavily populated areas of the Alps. This usually involves computing the characteristics of large return-period avalanches. Current tools (avalanche-dynamics or statistical models) cannot achieve this objective properly. A new generation of models has emerged, which, by combining statistical and deterministic viewpoints, can reduce a number of shortcomings in the original tools. This paper explores the possibility of updating the Salm–Burkard–Gubler method by adding a probabilistic procedure for fitting parameters to field data and using it in Monte Carlo simulations. The resulting model is intended to provide more accurate results of extreme avalanches. It has been applied to a series of close avalanche paths in the French Alps. Despite their similarities, these paths reveal some differences in their avalanche activity in terms of frequency and maximum run-out distance. Therefore, in order to provide a fair description of the intensity/frequency relationship, the model parameters must be fitted for each path, which leads to thinking that not all the important physical processes have been taken into account in this model.


*Keywords:* Monte Carlo simulation; Calibration; Avalanche

## 1. Introduction

The catastrophic avalanches of winter 1999 in Europe (Montroc, France, 12 deaths; Evoléne, Switzerland, 12 deaths; Galtür, Austria, 39 deaths) have renewed the interest in developing scientific methods for avalanche zoning. Basically, an engineer in charge of avalanche zoning at a given site wishes to estimate the avalanche deposit boundaries and potential impact pressure for large periods of return, typically equal to or larger than 100 years (Mears, 1992; Hopf, 1998).

In France, to determine the extent of extreme avalanches, practitioners use empirical methods, based on terrain analysis (study of vegetation for clues of past avalanches, analysis of aerial photographs, etc.), interview of residents, and archives. Like for any process relying on the experience of a few individuals (the experts), an approach of this kind suffers from unavoidable shortcomings even though it remains an indispensable step in any zoning: subjective character of the outcomes, phenomenon quantification delicate to obtain, etc. Lagging behind, scientific methods have so far received less attention in applications though

* Corresponding author. École Polytechnique Fédérale de Lausanne, Laboratoire d'Hydraulique Environnementale, Ecublens, 1015 Lausanne, Switzerland. Tel.: +41-21-693-3287; fax: +41-21-693-6767.

*E-mail address:* christophe.ancey@epfl.ch (C. Ancey).

0165-232X/$ - see front matter © 2004 Elsevier B.V. All rights reserved.
doi:10.1016/j.coldregions.2004.04.004

they would be helpful to improve the accuracy of empirical methods.

The objective of this paper is to propose a simple general framework for computing the magnitude–frequency relationship, with specific attention paid to extreme avalanches and the search for the largest applicability in engineering. Such an objective is not new since we count a large number of works devoted to this topic (Hopf, 1998). Here the main originality is that the magnitude–frequency relationship is deduced by mimicking the avalanche activity in a given path over long periods. To that end, we idealize the life of an avalanche by describing the main stages from snowfalls to run-out. This can seem more complicated than the usual approaches that mainly focus on the avalanche run-out but this makes it possible to introduce times series of meteorological data (e.g., intensity of snowfall, lag time between two snowfalls, etc.) in the model as input variables, which undoubtedly constitute the largest and widespread source of data to explain and predetermine the occurrence of avalanches. Using a more comprehensive framework for computing the magnitude–frequency relationship is largely justified by the failure of usual methods to obtain this relationship.

First we will begin the paper by explaining why the current avalanche models cannot provide proper evaluations of the magnitude–frequency relationship. We will then present the framework that we have tested. Most of the developments included in it are not new; the general scheme has been drawn from the method proposed by Salm et al. (1990), that we have adapted and updated to make it compatible with a probabilistic treatment. The calibration of the model parameter will be explained shortly; the reader is referred to a recent publication (Ancey et al., 2003). Finally, we will present the results obtained when applying the method to a series of avalanche paths in the Maurienne Valley (French Alps).

## 2. An overview of practical methods used in zoning

In addition to naturalist methods, there are currently two methods to deduce avalanches characteristics: the deterministic models (avalanche-dynamics models) and the statistical models. We are going to briefly present the two approaches. To illustrate the issues encountered when one tries to apply them to avalanche zoning problems, a typical example will also be studied. Note that here the problem at hand is not to test the reliability of general methods, such as the deterministic model proposed by Salm et al. (1990) or the statistical model developed by Lied and Bakkehøi (1980), but to address how field data can be used to deduce the behavior of extreme (usually not observed) avalanches. To make a parallel with modern hydrological treatments of rainfall data, our objective is to develop a theoretical framework that is able to deduce the behavior of extreme avalanches from the knowledge of past events similarly to extreme value theory for rainfall data (see Coles, 2001).

### 2.1. Deterministic models

Deterministic models reduce avalanche physics to a set of equations of motion, usually involving mass and momentum balance equations (Hutter, 1996; Ancey, 2001). The main criticism made of the current deterministic models is that they use ad hoc assumptions on the rheological behavior of snow (McClung and Schaerer, 1993). Despite various attempts to find physical justifications for their expressions (see, e.g., Salm, 1993), the constitutive relationships used so far rely on analogy with other physical phenomena: typical examples include the analogies with granular flows (Savage and Hutter, 1989; Savage, 1989; Tai et al., 2001), Newtonian fluids (Hunt, 1994), power-law fluids (Norem et al., 1986), and viscoplastic flows (Dent and Lang, 1982; Ancey, 2001). Nonetheless, even though all these new developments appear attractive from a physical viewpoint, from a purely rheological point of view they still rely on a speculative basis. Given the severe difficulties faced with snow rheometry, the physical calibration of constitutive parameters used in these models will remain unfeasible for a long time.

An alternative approach to fitting parameters involves comparing the model outputs and field data such as the velocity at a given point and the point of furthest reach (run-out distance) (Schaerer, 1974; Buser and Frutiger, 1980; Dent and Lang, 1980). The resulting fitted values have been proposed as default values in engineering guidelines such as the Swiss guidelines hereafter referred to as SBG method (Salm et al., 1990) or the USGS handbook (Mears,

1992). Although practitioners are generally confident of these values, recent studies have pointed out weaknesses in the values proposed by the current guidelines. For instance, when comparing the predictions of various deterministic models and field data on five European sites, Barbolini et al. (2000) have found that the friction parameter values could be very different from the default values. Another shortcoming when applying these models to avalanche zoning is that they do not explicitly include the notion of period of return, as is shown below. In the better cases, the period of return is implicitly introduced by setting the value of an input parameter to a given quantile. However, in a multivariate random process such as avalanches, the period of return should be computed from the joint probability of all the random variables involved in the problem and not exclusively from one of these variables otherwise this can lead to unrealistic return-period estimation (see Adamson et al., 1999 in the field of floods). In Appendix A, we provide evidence that, in the case of a sliding-block model, there are substantial differences between the periods of return computed on a single random variable or a set of variables.

Let us consider the case of the Folmeyan path in the Tarentaise valley (France), which regularly produces avalanches of any size. The path is an open north-facing slope whose starting zone is located on the Mont Pourri glaciers; the starting zone exhibits a complex structure, with at least three sub-basins that can operate more or less independently under critical conditions of snowcover unstability. The path is close

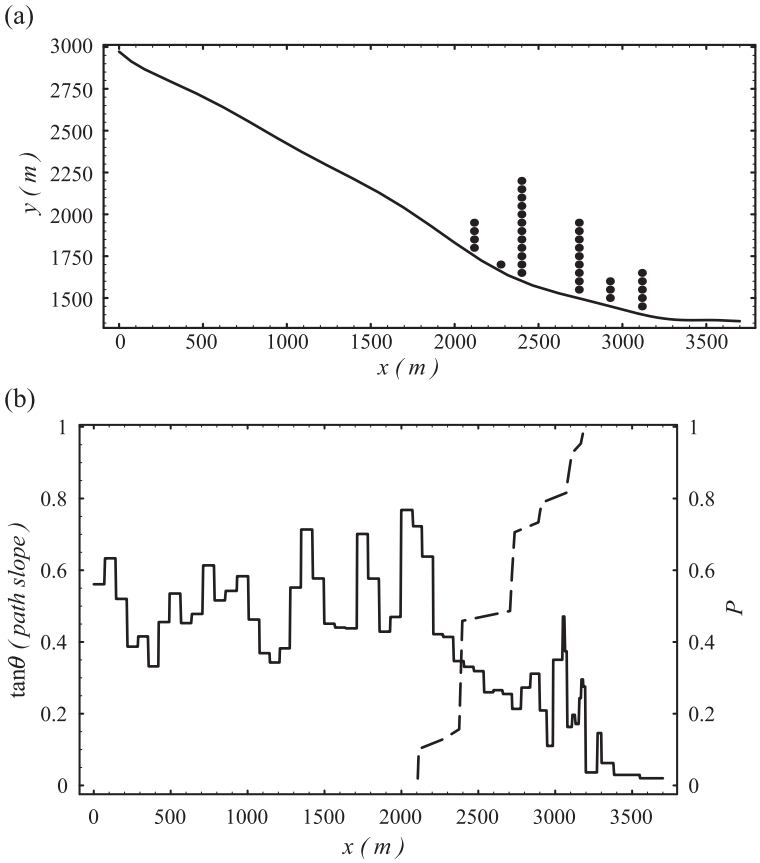


Fig. 1. (a) Path profile of the Folmeyan site. (b) Variation in the path slope as a function of the distance from the starting point (continuous line). Have also been superposed: the run-out distance distribution for all events in the avalanche database (in plot a) and the cumulative distribution function of the run-out distance $P$ (in plot b).

to Val d'Isère and is characterized by high annual snowfall rates (on average, 6.1 m from December to April at 2000 m). Several avalanches deposited close to a village (La Gurraz). The run-out elevation of large avalanches as well as other features (damage, volume, etc.) have been recorded since 1934. Fig. 1 reports the path profile (Fig. 1a) and the variation of the path slope with distance from the top point of the path (Fig. 1b). We have also superposed the recorded run-out distance. In Fig. 1a, each dot presents the run-out distance of each event recorded since 1934 while Fig. 1b reports the cumulative distribution of the run-out distance. Uncertainty on the run-out elevation is large, typically of the order of $\pm 25$ m for the older events while nowadays it should be closer to $\pm 10$ m. There is no guarantee as regards completeness of the database, notably during the last world war, a few events might be missing. Table 1 provides the dates and the run-out elevations for the last 22 events, for which the meteorological conditions before the release are known; meteorological data come from the meteorological station situated at Arc 2000 (elevation 2050 m, 2 km away from the starting zone). The table also reports the empirical cumulative probability $\hat{P}$ for each event; it is evaluated by sorting the run-out elevations (from smallest to largest). If $i$ is the value rank, $n$ is the number of field data (here $n=22$ from 1976), then $\hat{P}_i=(i-0.3)/(n+0.4)$.

Table 1
Event features in the Folmeyan path

| Date | Run-out elevation (m) | Distance (m) | $C_{3d}$ (cm) | $\mu$ | $\hat{P}$ |
|---|---|---|---|---|---|
| 04/02/1980 | 1500 | 2740 | 115 | 0.26 | 0.70 |
| 05/01/1981 | 1600 | 2400 | 78 | 0.36 | 0.43 |
| 12/03/1981 | 1650 | 2275 | 30 | 0.35 | 0.13 |
| 31/03/1981 | 1500 | 2740 | 65 | 0.25 | 0.54 |
| 23/01/1984 | 1380 | 3195 | 67 | no solution | 0.95 |
| 25/02/1985 | 1600 | 2400 | 0 | – | 0.16 |
| 20/05/1985 | 1600 | 1400 | ? | ? | 0.38 |
| 16/01/1986 | 1400 | 3115 | 31 | no solution | 0.93 |
| 14/02/1990 | 1380 | 3195 | 154 | 0.2 | 0.97 |
| 15/02/1992 | 1600 | 2400 | 49 | 0.35 | 0.29 |
| 06/04/1993 | 1500 | 2740 | 66 | 0.25 | 0.57 |
| 01/01/1994 | 1500 | 2740 | 37 | 0.24 | 0.51 |
| 10/04/1994 | 1600 | 2400 | 49 | 0.35 | 0.35 |
| 25/01/1995 | 1450 | 2925 | 98 | 0.24 | 0.76 |
| 15/02/1995 | 1500 | 2740 | 24 | 0.23 | 0.49 |
| 25/02/1995 | 1450 | 2925 | 147 | 0.25 | 0.79 |
| 09/02/1999 | 1600 | 2400 | 107 | 0.37 | 0.46 |
| 22/04/1999 | 1600 | 2400 | 21 | 0.35 | 0.18 |
| 25/12/1999 | 1600 | 2400 | 45 | 0.35 | 0.27 |
| 04/03/2001 | 1600 | 2400 | 36 | 0.35 | 0.24 |
| 21/03/2001 | 1600 | 2400 | 14 | 0.35 | 0.21 |

Dates, run-out elevation and distance, snow fallen during the previous 3 days, and the fitted value of $\mu$ (with $\xi=1000$ m/s$^2$), and the cumulative distribution function $P$ of the run-out distance.

We are interested in applying a Voellmy-like method (see Section 3.4 for details) to deduce the traits of extreme avalanches in the Folmeyan site. The first task is to evaluate the two friction coefficients ($\mu$ and $\xi$) involved in this model. The first problem is that we only dispose of one type of avalanche data (run-out elevation) to adjust the two parameters. According to the SBG scheme, in addition to the initial flow depth, the only varying parameter is the friction coefficient $\mu$ since it is interpreted as something close to snow viscosity while the second coefficient $\xi$ reflects the "geometrical" resistance exerted by the path on the avalanche and, thus, is independent of avalanches. Thus, assuming $\xi$ constant and setting it to a given value, we can fit the parameter $\mu$ for the computed run-out elevation to match the observed value. This can be done for different values of $\xi$ in order to have an idea of the sensitivity in the dependence of $\mu$ on $\xi$. Usually, if one keeps the range of values given in the SBG guidelines (that is, $400\leq\xi\leq1000$ m/s$^2$), this dependence is weak.

Table 1 provides the values of $\mu(C_{3d}|\xi=1000)$ for the avalanches occurred since 1976, where $C_{3d}$ denotes the amount of snow fallen during the previous 3 days (not including the day where the avalanche descended), which is computed by summing the amounts of snow recorded daily (from 8:00 to 8:00 the day after). Fig. 2 shows the variation of the run-out distance with the snow fallen during the previous 3 days $C_{3d}$. On the whole there is no clear relationship between the run-out distance $x_{stop}$ and $C_{3d}$. If we consider heavy snowfalls by limiting our attention to snowfalls in excess of a given threshold, e.g. 70 cm, the data define a trend which could be approximated by eye as a rapid increase of the run-out distance with $C_{3d}$. However, possibly as a result of observation inaccuracies (in the avalanche date, run-out distance, and snowfall measurement), the data scatter so widely that this increase represents only a gross qualitative trend, from which a linear/nonlinear behavior cannot even be made discernible. This trend is consistent with the fact that the probability of observing long

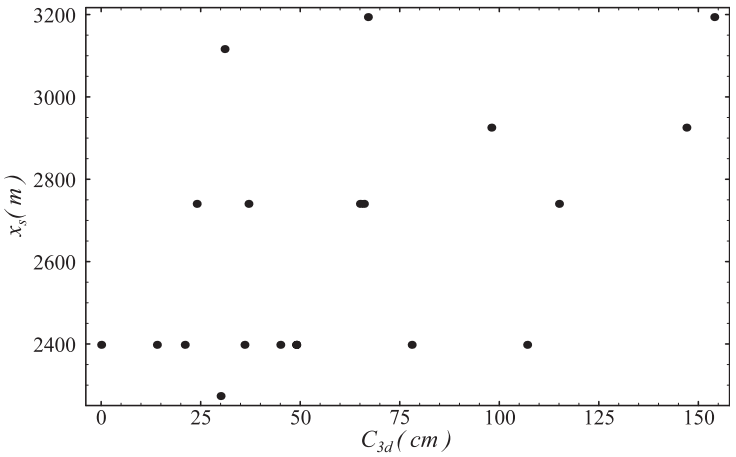


Fig. 2. Variation in the run-out distance as a function of the snow amount fallen during the previous 3 days for the Folmeyan site.

run-out distances increases with the amount of new snow. In some cases, the avalanche travelled a very long distance although the recent snowfall was low (e.g., avalanche of 16 January 1986 in Table 1). This may be seen as an odd behavior at first sight, but various explanations can be evoked.

- If the variable $C_{3d}$ appears often as a critical parameter in the assessment of avalanche activity, there is no strict determinism between the release probability and $C_{3d}$ because major avalanches can be released after snowfalls that were not necessarily intense but sustained over several days. For instance, the avalanche of 16 January 1986 occurred at the end of a period of bad weather conditions lasting a couple of weeks, for which the sum of daily snowfalls reached 205 cm from 1 January to 16 January 1986, with a maximum of 34 cm/day recorded on 11 January 1986.
- Avalanche mobility varies substantially depending on snow consistency, snowcover strength, path smoothness, etc. Small volume avalanches can exceptionally travel long distances when basal friction and energy dissipation within the avalanche are low. A typical example was provided by the Daille path (Val d'Isère), a few kilometers distant from the Folmeyan path, where three backcountry skiers were buried on 23 February 1996 by a small avalanche naturally released after a light snowfall (16 cm in 3 days, temperature ranging from $-16$ °C to $-10$ °C) (Ancey, 1998). This avalanche was exceptional because it travelled a very long distance compared to its usual extent and was the sole event observed in Val d'Isère over the last 10 days.

In short, we failed to identify a one-to-one relationship between the run-out distance and the snow falls despite the evident influence of snowfall intensity on the run-out distance for heavy snowfalls. If we look at the $C_{3d}$ dependence of the friction coefficient $\mu$, we arrived at the conclusion: there is no clear relation between $\mu$ and $C_{3d}$. This means that the $\mu$ dependence on $C_{3d}$ should be expressed in probabilistic terms and not through a deterministic relationship.

When taking a closer look at Table 1, we notice that $\mu$ takes its values over a finite set of possible values; typically here, we have: $\mu=0.2$, $\mu=0.24-0.27$, or $\mu=0.35-0.37$. The fact that we do not find a continuous distribution of $\mu$ values can result from preferential points of run-out (see Fig. 1a). Surprisingly, the $\mu$ probability distribution is smoother if a Coulomb expression is selected for the frictional force instead of the Voellmy expression (or, in other words, if we set $\xi=0$) (Ancey, in press).

We have been successful in fitting the Voellmy-like model parameters for most avalanches occurred over the last 20 years. How can this adjustment be used to deduce the features of extreme avalanches? Due to the absence of dependence between variables, we have no sound argument for selecting a given value of $\mu$. Thus, the Voellmy model cannot provide an accurate esti-

mate of the run-out distance of the 100-year avalanche. Note that this problem is avoided in the SBG method by imposing that the 100-year avalanche results from a 100-year snowfall (more precisely, an increase in snowcover thickness over 3 days, whose return period is 100 years).

### 2.2. Statistical models

In the black-box approach, no explicit attempt is made to capture the physics of processes involved. Approaches of this kind are quite common in hydrology (O'Connell and Todini, 1996), but are less frequent in snow hydrology. In this field, the basic idea stems from the pioneering work of Lied and Bakkehøi (1980): assuming a regional homogeneity in avalanche behavior for a given mountain range, they pooled the data from various paths in a common database. In this way, using regression techniques, they obtained the relationship between the run-out distances and a number of key variables of the path profile. This methodology has been applied to different mountain ranges throughout the world (Bakkehøi et al., 1983; McClung and Lied, 1987; Fujizawa et al., 1993) and extended to introduce the period of return as a parameter of the problem (McClung, 2000, 2001). In alpine countries, where most of the time the avalanche paths of the same mountain range exhibit no similarity in their shape, the fundamental assumption of avalanche homogeneity on a regional scale is doubtful (Ghali, 1996). A major drawback of this approach is that it depends a great deal on the quantity and quality of available data. Since most of the time the only available information is the run-out distance, this approach is unable to provide estimates of the potential impact pressure. Moreover, in many cases, the historical record of run-out distances is not long enough and the resulting fitted probability distribution must be extrapolated to evaluate the run-out distance of a long return-period avalanche. However, extrapolation is far from easy and proper due to the non-smoothness of the distribution and dependence of run-out distance on path profile; here mathematical theories such extreme value theory (Coles, 2001) cannot be applied to extrapolate field data.

Let us illustrate this with the Folmeyan site example. The avalanche database has been recording 22 events for 25 years. We are interested in determining the run-out distance of the 100-year avalanche. We admit that the period of return of the avalanche $T$ can be computed from the run-out distance. The 100-year runt-out distance is the value (quantile) at which the cumulative distribution function reaches $P = 1 - T^{-1} = 0.99$. In Fig. 1, we have reported the variation in the empirical distribution of $x_{\text{stop}}$. By interpolating points corresponding to the 22 events, we can obtain an estimate of $P$ in the range 0–0.97. A priori, it could seem easy to extrapolate the empirical curve up to 0.99. This is, however, a difficult task since the curve is step-shaped and from a mathematical viewpoint there is no way to properly extrapolate it.

This result is not surprising: it is well known in hydrology that, in order to obtain correct statistical estimates, one has to select *physical* variables, i.e. variables independent of the path geometry. For instance, in flood hydrology, a bad choice of statistical variable would be the flow depth since it depends a great deal on the river cross-section shape: if the river sides are steep, any increase in water discharge leads to a measurable increase in the flow depth but, if the river flanks flatten out, the flow depth increase resulting from a discharge rise is low.

Here statistical methods are thus of little help for zoning applications since they can interpolate data, but cannot be used to predict rare events. Therefore, unless one has very long series of data, it is not possible to properly evaluate the 100-year avalanche features.

## 3. A minimalist conceptual framework

In-between these two classic approaches has emerged a new class of models that can be referred to as *conceptual models* since they rely on an *idealized representation* of avalanches and encompasses a number of varied tools coming from statistics, physics, and naturalist knowledge of avalanches. Conceptual models are common in hydrological applications (O'Connell and Todini, 1996); in this respect, it is worth mentioning that our objective (determining the run-out distance and pressure of avalanches using meteorological data) is not so far from the one followed by the methods of rainfall/flow-rate transformation (determining the water discharge in a stream from the rain data). Thus, in the following, "idealized representa-

tion'' means that we do not pretend that our representation is systematically physical but merely that it describes roughly what happens.

### 3.1. Outline

Conceptual models can be viewed as the combination of different modules (or sub-models) describing the different processes occurring from snowfalls to avalanche deposition. Due to the large complexity in the elementary processes and their interplay, this combination is nothing but an idealized mathematical description of the steps believed to be crucial in the release and course of avalanches.

The structure of the model is conditioned by the number and nature of the measurable physical data at hand. To build up our conceptual model, we first need to reply to the following basic questions:

- What are we looking for? The magnitude-frequency relationship of key dynamic variables of avalanche at a given site, that is, the probability of observing a given value of the key dynamic variable(s). Therefore, our model must take probabilistic aspects into account. The dynamic variables of interest depend on the problem to treat. In zoning, we are mainly interested in the deposit extension and the maximum pressure variation along the avalanche path. Since the avalanche pressure distribution cannot be easily measured, we need a practical way to evaluate it. Avalanche-dynamics models are potentially good candidates for this purpose.
- What kinds of data are usually available? In the French Alps, the only continuous source of data related to avalanches is constituted by the meteorological databases. For a number of sites in the heavily populated valleys, we have some indications of the run-out elevation of past avalanches. Exceptionally, for a few events, it is possible to have an idea of the volume of snow involved, maximum pressure, and velocities from analysis of damage to forest, records, testimonies, etc. Thus, for a model to be applicable in any site, the input parameters must be related to the meteorological data while other sources of information can be used to adjust inner parameters of the model.

Various combinations of modules have been explored by different authors (Keylock et al., 1999; Barbolini and Savi, 2001; Bozhinskiy et al., 2001; Chernouss and Fedorenko, 2001; Harbitz et al., 2001; Keylock and Barbolini, 2001). Our opinion is that when the objective is to mimic the avalanche activity over long periods, conceptual models should be based on Monte Carlo simulations and, at least, two sub-models: one to quantify the occurrence of avalanche release and another to compute the avalanche motion and deposition. Here, we use classic hydrological methods for describing the occurrence and intensity of snowfall and, as regards avalanche motion, we have adapted and updated the SBG method. The main difference between the present framework and the original formulation of the SBG method is that we use a probabilistic method for fitting the parameters. If a formal relationship between the probability density functions of conceptual and observable variables can be established, then the model can be easily calibrated. In this way, even short series of field data can be used insofar as it is possible to properly define their probability density function.

The avalanche-dynamics sub-model used is very close to the Salm-Burkard-Gubler (SBG) model, except that the approximate method of solving the equations of motion has been replaced by an ordinary differential equation, solved numerically. In its original formulation, the Voellmy model belongs to the class of sliding-block models, which present the advantage of leading to simple ordinary differential equations, but also the drawback of overly simplifying the physics of avalanches. Disadvantages and advantages offered by Voellmy-like models are discussed in a number of recent papers and monographs (McClung and Mears, 1995; Bartelt et al., 1997, 1999), to which the reader can refer. More refined models have been developed over the last two decades. Among others Eglit (1983, 1984, 1998), Bartelt et al. (1997) and Barbolini and Savi (2001) have included the Voellmy frictional force in the flow-depth averaged equations of motion (similar to shallow water equations used in hydraulics), leading to a set of hyperbolic partial differential equations. Several reasons have led us to use a Voellmy-like model despite its limitations:

- First of all, this model, notably in the formulation known as the Salm-Burkard-Gubler (SBG) model,

is widely used in Europe for avalanche zoning and engineering. Its success stems from this model's long history (the first sliding block-model seems to date back to the 1920s, Mougin, 1922) and its simplicity. The method proposed here provides the practitioner with the means to tune the model parameters from field data.

- Furthermore, the avalanche-dynamics model is an element of the chain needed to model the physical processes from snowfall to avalanche deposition. At this stage, we are mainly interested in finding a simple mathematical model rather than a sophisticated model, which would be time-consuming and involve many parameters. Based on an ordinary differential equation and two mechanical parameters, the SBG method plainly fulfills our objective. More refined evolutions of this model, relying on hyperbolic partial differential equations, are more complicated to handle and a number of assumptions (long-wave approximation, stability, front, etc.) limit their applicability.

### 3.2. Structure of the model

Our minimalist conceptual model includes two modules (see Fig. 3):

- The first module describes what happens up to the avalanche release. The avalanche release is largely conditioned by the meteorological conditions during the previous days, especially the amount of new snow (McClung and Schaerer, 1993; Ancey, 1998). For many sites, the key meteorological parameter explaining an avalanche activity is the sum of the amount of snow fallen during the previous 3 days $C_{3d}$. Not all the sustained snowfalls give rise to avalanche. Thus, for a given snowfall $C_{3d}$, one has to specify the probability of observing an avalanche release $p(\text{release}|C_{3d})$. The 3-day snowfall $C_{3d}$ and the lag between two snowfalls $\tau$ are random variables. Their probability density functions $p_C(C_{3d})$ and $p_\tau(\tau)$ can be estimated using classic hydrological methods (renewal, annual series methods, etc.). Usually an extreme-value distribution (Fréchet, Weibull, or Gumbel distribution) or an exponential distribution provides good results while a Poisson law can be used to evaluate the number of snowfalls per time unit exceeding a given threshold. Evaluation of $p(\text{release}|C_{3d})$ is simply achieved using logistic regression techniques (Hosmer and Lemeshow, 1986).
- The second module describes avalanche motion and deposition. Here we use an avalanche-dynamics model. This takes the form of a set of dynamical equations, basically the mass and momentum balance equations describing the time variations of dynamical variables of avalanche motion, here the velocity $u$ and flow depth $h$. The equations of motion depend on a set of mechanical parameters $\{\mu,\xi\}$, specified hereafter (Section 3.4).

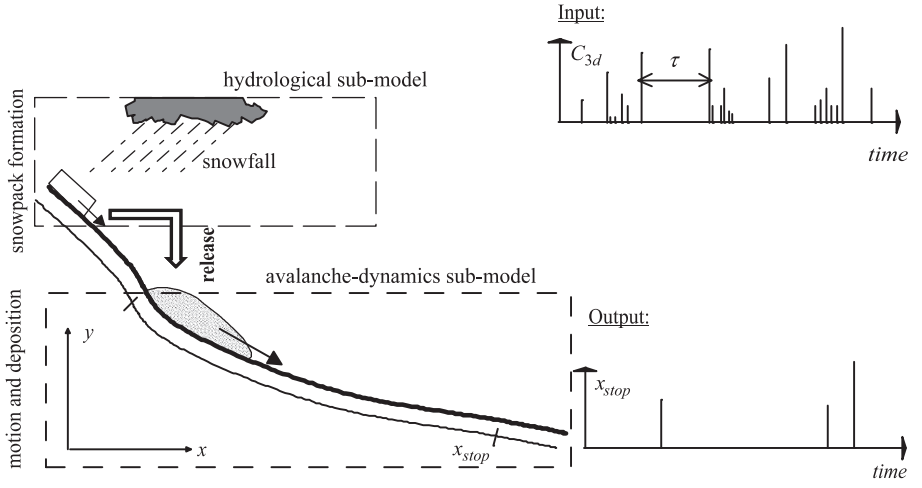


Fig. 3. Sketch of the conceptual model used here.

With these two modules, we are able to compute the run-out distance $x_{stop}$ provided that the initial conditions are known and the mechanical parameters are specified. This also implies that there is a known dependence between the 3-day snowfall and the initial conditions for the equations of motion. In the following, we express the functional dependence of the run-out distance $x_{stop}$ on $\{\mu,\xi\}$ and $C_{3d}$ as follows: $x_{stop}=Y(C_{3d};\xi,\mu)$.

### 3.3. Model calibration

Though conceptual models erase some of the intrinsic disadvantages of fully deterministic and statistical approaches, they must still cope with a difficult problem: the calibration of parameters using the scarce physical data available. For instance, due to the lack of long series of data, Barbolini and Savi (2001) and Barbolini et al. (2003) collected data from several paths to deduce the probability density functions of the two parameters involved in their propagation sub-model. Alternative methods, which are not based on a regionalization assumption, can be used. Here we propose a probabilistic method which tries to deduce the relationship between the probability distributions of input and output variables.

The basic question in the inverse problem is: given $x_{stop}$ and $C_{3d}$, what are the values of the mechanical coefficients $\{\mu, \xi\}$? If we can invert the function $Y$, one can deduce a single mechanical parameter from the field data $x_{stop}$ provided that the other mechanical parameter is known: $\mu=Y^{-1}(x_{stop};C_{3d}|\xi)$. This simple technique requires knowing $x_{stop}$ and $C_{3d}$ precisely for each event. This difficulty can be alleviated if we consider the problem differently. Indeed, rather than solving the equation $\mu=Y^{-1}(x_{stop};C_{3d}|\xi)$ for each event, we can solve it globally. To be more specific, we now formulate the inversion problem in the following manner: given the probability distributions of $x_{stop}$ and $C_{3d}$, what is the probability distribution of the coefficient $\mu$? We will refer to this formulation as the *indirect method*.

To answer the question above, we shall consider three different assumptions: (i) the random variables $\mu$ and $C_{3d}$ are independent, (ii) they are linked by a one-to-one relationship in the form $\mu=F(C_{3d})$, (iii) they are correlated random variables. Theoretically, the marginal density of the friction coefficient is given by:

$$\begin{aligned} p_\mu(\mu) &= \int_{\mathbb{R}+} \mathrm{d}x_{stop} \int_{\mathbb{R}+} \mathrm{d}C_{3d} P[\mu \,|\, x_{stop}, C_{3d}] P[x_{stop}, C_{3d}] \\ &= \int_{\mathbb{R}+} \mathrm{d}x_{stop} \int_{\mathbb{R}+} \mathrm{d}C_{3d} P[x_{stop}, C_{3d}] \delta(\mu - Y^{-1} \\ &\quad \times (x_{stop}; C_{3d} \,|\, \xi)), \end{aligned}$$

but this equation is to intricate to be used in numerical computations. We proceed as follows. Let us consider the marginal density of the run-out distance:

$$p_x(x_{stop}) = \int_{\mathbb{R}+} p_{x,\mu}(x_{stop}, \mu)\mathrm{d}\mu \tag{1}$$

It is possible to remove the variable $x_{stop}$ in the joint probability by making a variable change: $(x_{stop},\mu)$ to $(C_{3d},\mu)$. We denote $J_x$ the Jacobian of this transformation:

$$J_x = \left| \det \begin{bmatrix} \partial x_{stop}/\partial C_{3d} & \partial x_{stop}/\partial \mu \\ \partial \mu/\partial C_{3d} & \partial \mu/\partial \mu \end{bmatrix} \right| \tag{2}$$

Formally, we then obtain the marginal density of $x_{stop}$:

$$\begin{aligned} p_x(x_{stop}) &= \int_{\mathbb{R}+} p_{x,\mu}(x_{stop}, \mu)\mathrm{d}\mu \\ &= \int_{\mathbb{R}+} J_x^{-1} p_{C,\mu}(C_{3d}, \mu)\mathrm{d}\mu \end{aligned} \tag{3}$$

The next task is to extract the probability density of $\mu$ from this integral expression. Said differently, we are trying to invert the integral term to provide an expression of $p_\mu(\mu)$ as a function of $p_x(x_{stop})$ and $p_C(C_{3d})$. Different cases must be considered.

#### 3.3.1. Case (i): independency of $\mu$ and $C_{3d}$

If $\mu$ and $C_{3d}$ are independent random variables, then we have: $\partial\mu/\partial C_{3d}=0$, $J_x=|\partial x_{stop}/\partial C_{3d}|$,

and $p_{C,\mu}(C_{3d},\mu)=p_C(C_{3d})p_\mu(\mu)$. Thus the marginal probability density function of the run-out distance is obtained by integration:

$$p_x(x_{stop}) = \int_{\mathbb{R}+} J_x^{-1} p_C(C_{3d}) p_\mu(\mu) \mathrm{d}\mu \tag{4}$$

If we further assume that $x_{stop}=Y(C_{3d};\mu|\xi)$ can be inverted to yield $C_{3d}=Y^{-1}(\mu;x_{stop}|\xi)$, we deduce that the probability distribution $p_\mu$ satisfies a Fredholm equation of the first kind:

$$p_x(x_{stop}) = \int_{\mathbb{R}+} K(x_{stop},\mu) p_\mu(\mu) \mathrm{d}\mu \tag{5}$$

where $K(x_{stop},\mu)=J_x^{-1} p_C\,(Y^{-1}(\mu;x_{stop}|\xi))$ is the kernel function.

*3.3.2. Case (ii): deterministic dependency of μ on $C_{3d}$*

If there is a one-to-one relationship between $\mu$ and $C_{3d}$ in the form $\mu=F(C_{3d})$, the result is straightforward:

$$p_\mu(\mu) = \frac{1}{|F' \circ F^{-1}(\mu)|} p_C(F^{-1}(\mu)) \tag{6}$$

*3.3.3. Case (iii): correlated behavior of μ and $C_{3d}$*

Instead of a deterministic relationship between $\mu$ and $C_{3d}$, we can imagine that the two variables are correlated. We follow the same line of reasoning as above, except that we consider conditional probability densities:

$$\begin{aligned} p_x(x_{stop}\,|\,C_{3d}) &= \int_{\mathbb{R}+} P[x_{stop},\mu\,|\,C_{3d}]\mathrm{d}\mu \\ &= \int_{\mathbb{R}+} P[x_{stop}\,|\,\mu,C_{3d}]P[\mu\,|\,C_{3d}]\mathrm{d}\mu \end{aligned}$$

Using the fact that $P[x_{stop}|\mu,C_{3d}]=\delta(x_{stop}-Y(\mu,C_{3d}))$, we can write:

$$p_x(x_{stop}\,|\,C_{3d}) = \int_{\mathbb{R}+} K(x_{stop},\mu\,|\,C_{3d}) P[\mu\,|\,C_{3d}]\mathrm{d}\mu \tag{7}$$

where $K(x_{stop},\mu|C_{3d})=\delta(x_{stop}-Y(\mu,C_{3d}))$ is the kernel function. In this case, we do not compute $p_\mu$, but the conditional probability $P[\mu|C_{3d}]$.

*3.3.4. Summary and numerical solving*

Except for case (ii), where the probability density of $\mu$ is directly inferred from that of $C_{3d}$, we have found that the marginal density of $\mu$ [see case (i)] or the conditional density $P[\mu|C_{3d}]$ [see case (iii)] are solutions to a Fredholm equation in the form: $p_x=\int d\mu\ K\ (\mu,x_{stop})P_\mu$.

There is usually no analytical solution to this equation. To solve numerically this equation, the basic idea is to discretize the integral equation to obtain a matrix form that can be inverted: $p_\mu=K^{-1}P_x$. Different numerical methods can be used to discretize and solve a Fredholm equation (e.g. see Kirsch, 1996). We have used the Tikhonov regularization method, which reduces fluctuations of the discretized solution by imposing a constraint on the smoothness of the solution. The complete numerical implementation is explained in a recent paper (Ancey et al., 2003). In the Tikhonov method, we can use different regularization methods: for instance, we can constraint the curve to be smooth (denoising process) or limit overly large fluctuations. In this method, there is also an adjustable factor that controls the extent to which the resulting curve is smooth or close to experimental data. In practice, this free parameter allows one to find a good compromise between agreement and smoothness (or stability relative to variations in the data).

The major problem of Tikhonov regularization methods is the robustness and sensitivity of results to the choice of the smoothing operator and measurement errors. An alternative is to use Markov Chain Monte Carlo simulations to obtain a sample of values drawn from the marginal density $p_\mu$; Ancey (in press) used such a method to deduce the probability density of $\mu$ for various paths in the French Alps.

In the remaining of the paper, we will use the assumption that $\mu$ and $C_{3d}$ are independent random variables [case (i)].

### 3.4. The avalanche-dynamics model

In the computations presented here, we have used the Salm-Burkard-Gubler formulation of the Voellmy model. The SBG model relies on momentum and mass balance equations for describing avalanche motion (Salm et al., 1990; Salm, 1993). Motion is described within the framework of rigid-body mechanics. The

momentum equation is expressed as follows: $m\dot{u} = mg\sin\theta - F$, where the dot means the time derivative, $\theta$ is the path inclination, $m$ is the avalanche mass, $u$ its velocity, and $F$ is the friction force experienced by the avalanche. For an unconfined avalanche, this force has the form: $F = \mu mg\cos\theta + mgu^2/(\xi h)$, where $h$ refers to the flow depth, $\xi$ and $\mu$ are two friction coefficients. The mass balance equation expresses that the mass flow rate $Q$ holds constant throughout the run: $Q = \rho lhu = \rho_0 l_0 h_0 u_0$, where the subscript 0 refers to the initial conditions (i.e., at the end of the release phase), $l$ denotes the avalanche width, and $\rho$ its density. For confined flows, the flow depth must be replaced by the hydraulic radius $R_h = S/\chi$ (where $S$ denotes the flow cross-section area and $\chi$ is the wetted perimeter, namely the length of the cross-section border at the interface between the avalanche and the ground/snowcover) in the frictional force expression above.

The SBG method involves four input parameters:

- the initial conditions $h_0$ and $u_0$,
- the friction parameters $\xi$ and $\mu$.

It is assumed that the initial velocity (at the end of release phase) is: $u_0 = \sqrt{\xi h_0 \cos\theta_0 (\tan\theta - \mu)}$ (Salm et al., 1990), where $\theta_0$ denotes the mean slope of the starting zone. The initial flow depth $h_0$ corresponds to the thickness of the released snow layer. Here it is assumed that this thickness is directly correlated with the amount of snow fallen during the previous 3 days $C_{3d}$: $h_0 = f(\theta_0) C_{3d}$, where $f(\theta_0) = 0.291/(\sin\theta_0 - 0.202\cos\theta_0)$; this expression differs slightly from the original proposed by Burkard and Salm (1992) in that it takes into account $C_{3d}$ and not the growth rate $\Delta H_{3d}$ of the snowcover over 3 days (the difference in snowcover thickness over 3 days). Burkard and Salm (1992) also suggested increasing $\Delta H_{3d}$ to account for possible wind effects and/or elevation difference between the starting zone and the meteorological station.

The friction coefficient $\xi$ reflects the effect of path roughness. It is assumed to range from 400 to 1000 m/s$^2$ and be intrinsic to the path, that is, it is constant for each avalanche run in a given path. In contrast, $\mu$ pertains to snow fluidity. This parameter may depend on the avalanche size and/or other parameters. Its lower value given in the literature is 0.155 and corresponds to extreme avalanches (Buser and Frutiger, 1980).

In short, we have three effective input parameters ($\xi$,$\mu$,$C_{3d}$), two of which can be considered as random variables ($\mu$,$C_{3d}$) while the third ($\xi$) can be assumed to be constant (for a given site).We found no clear evidence in the literature for the last assumption. We have found that, insofar as we are involved in working with $x_{stop}$ and we constrain $\xi$ to lie within the prescribed range of 400–1000 m/s$^2$ (Salm et al., 1990), the precise determination of $\xi$ is of less importance since $x_{stop}$ usually depends weakly on $\xi$. Therefore, as a first approximation, it is permissible to make the calculation as if $\mu$ were really independent of $\xi$. However, if one leaves the SBG framework, that is, if $\xi$ can take any real value, the indirect inversion method will provide the conditional probability density function $p_\mu(\mu|\xi)$.

### 3.5. Practical use

In practice, the proposed method can be broken down into different steps (see Fig. 3):

(1) Calibration step: field data (snowfall, run-out distances, etc.) are used to obtain the release probability and the probability distribution of the friction coefficient $\mu$. Release probability can be estimated using regression logistic tools. The density distribution of $\mu$ can be evaluated using the *indirect method* presented here. This method benefits from posing the inverse problem in a probabilistic perspective. Moreover it allows us to compute the coefficient $\mu$ even though we have partial series of $x_{stop}$ or $C_{3d}$. Finally, it is especially suitable for Monte Carlo simulations, for which the $\mu$ values are generated from their probability density function $p_\mu(\mu)$. Its major inconvenience lies in the excessive sensitivity of results to measurement errors. An alternative is to use Markov Chain Monte Carlo simulations to generate $p_\mu$ (see Ancey, in press).

(2) Simulation step: Monte Carlo simulations are used to reproduce the avalanche activity:
   - The snowfalls are randomly generated: we draw the lag $\tau$ between two snowfalls from its distribution $p_\tau$ and the snow fall intensity $C_{3d}$ from $p_C$.
   - The probability release $p(\text{release}|C_{3d})$ is estimated. A random number $r$ is drawn

from a uniform distribution $p_{[0,1]}$. If $r>p$ (release$|C_{3d}$) there is an avalanche release. If there is no release, we go back to the first stage of the loop.

- The friction coefficient $\mu$ is drawn from its empirical distribution (this may be a difficult task, involving specific methods such as the rejection sampling algorithm, see Press et al., 1992; Gilks, 1996; Robert, 2001). An avalanche-dynamics model is used (such as the Voellmy-like model presented here). The dynamical features of the avalanche are stored.
- The process is iterated as long as is required.

(3) Extreme avalanche estimation: since we have generated long time series of avalanche data, it is possible to compute the period of return based either on the marginal density of the run-out distance or any combination of input/output variables.

This scheme presents obvious similarities with other Monte Carlo models (Harbitz et al., 2001; Barbolini et al., 2003; Meunier and Ancey, in press). Compared to these models, the presented framework aims at reproducing the different processes from snowfall to avalanche deposition, including meteorological conditions, snowcover stability, and avalanche dynamics. The sub-models are independent, which makes it possible to easily adapt the framework. For instance, if air temperature is assumed to be a critical parameter in avalanche release, it is

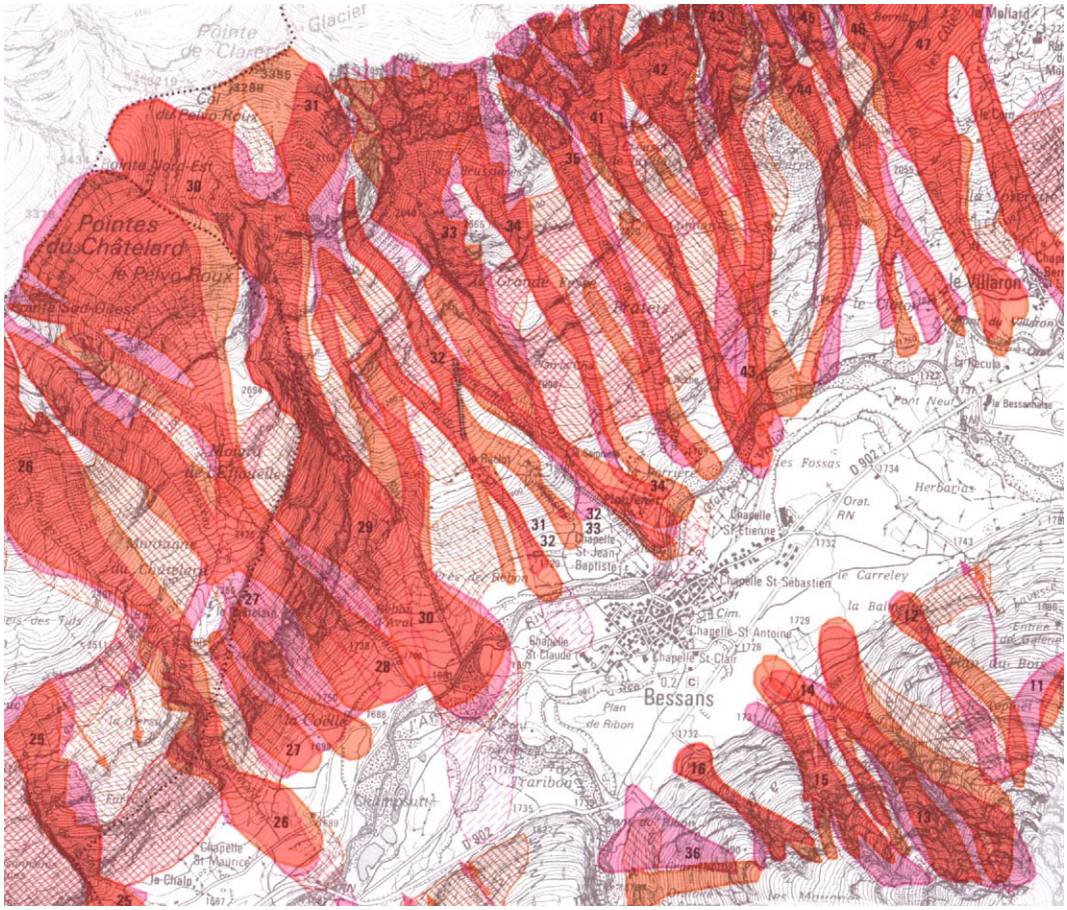


Fig. 4. Avalanche map of Bessans. © Cemagref-IGN (1992).

possible to account for it in the simulations. Another advantage of this framework is the possibility to vary the path profile with time. Indeed, a number of fatalities result not from the occurrence of a single event, but from the close occurrence of several events, each avalanche leading to a significant modification in the path profile. The deposit of a previous avalanche can smooth the path profile or deviate the flux of another avalanche. Such an ingredient can be taken into account here since each simulated event is associated with an occurrence date.

## 4. Application

We have applied the proposed method to a series of paths at Bessans in the Maurienne valley (French Alps, Savoie). We have selected these sites because they have experienced a large avalanche activity over the last century. The avalanche database is called the *Enquête Permanente des Avalanches* (permanent avalanche survey). Fig. 4 is drawn from the Carte de Localisation des Phénoménes d'avalanches (CLPA) [avalanche phenomenon localization map] and shows the avalanche paths surrounding Bessans and Table 2 provides the main features of the selected paths.

We will begin by presenting the typical results obtained with a single path. We will then summarize the results obtained on all the paths studied here. Only the results related to the calibration step will be presented in this section.

Table 2
References and main characteristics of the studied avalanche

| EPA ref. | CLPA ref. | Orientation | Event number | Elevation range (m) |
|---|---|---|---|---|
| 12 | 41 | south | 109 | 1700–3000 |
| 13 | 35 | south | 59 | 1700–3000 |
| 14 | 34 | south | 65 | 1700–2700 |
| 15 | 33 | south | 95 | 1725–3250 |
| 16 | 32 | south | 127 | 1700–3100 |
| 17 | 30 | south | 101 | 1700–3050 |
| 27 | 14 | north–west | 68 | 1700–2900 |
| 38 | 22 | north | 52 | 1700–2825 |
| 46 | 28 | south–east | 56 | 1750–3250 |

Here are provided the EPA reference, the CLPA reference, the overall orientation to the sun, the number of events occurred since 1901, and the range of elevation above the sea level.

### 4.1. Detailed analysis of a path

The test site is path EPA 16, in the south-eastern face of Pointe de Claret. The path extends between 3150 and 1700 m in elevation for a total length exceeding 2.1 km. The cross-section is very irregular: the middle part of the path is confined in a steep and curly gully while both the starting zone and the deposition are wide unconfined surfaces. Since 1901, 127 avalanches have been documented. Fig. 5 reports the empirical cumulative distribution function of the run-out distance together with the path slope profile. The meteorological station (1710 m), 2.5 km from the starting zone, has been recording snow data since 1981. Using the *peak over threshold* method (Coles, 2001), we have found that the probability of observing a snowfall $C_{3d}$ over 3 days is:

$$p_C(C_{3d}) = \exp\left(-\frac{1}{17.95}\frac{C_{3d}-47.5}{18.6}\right) \tag{8}$$

The maximum 3-day snowfall is described by: $C_{3d}=47.5-18.6\ \ln(-\ln(1-T^{-1}))$ ($C_{3d}$ expressed in centimeters, $T$ in years). The release probability was found to be:

$$p(\text{release}\,|\,C_{3d}) = \frac{\exp(-5.0450+0.039C_{3d})}{(1+\exp(-5.0450+0.039C_{3d}))} \tag{9}$$

The logit function is expressed as: $\ln(p(\text{release}|C_{3d})/(1-p(\text{release}|C_{3d})))=-5.0450+0.039C_{3d}$. The Hosmer-Lemeshow test yields 0.69 while the Pearson test provides 0.98.

We have also examined other combinations of meteorological parameters to provide better correlations between the meteorological conditions (during the days preceding the avalanche) and the avalanche occurrence. As meteorological indicators, we have used: the amount of snow fallen during the previous 3 days (not including the avalanche day) $C_{3d}$, the amount of snow fallen the day before the avalanche $C_{1d}$, the maximum temperature (recorded at 1700 m during the avalanche day) $T_{max}$, the average temperature $T_{mean}$, the minimum temperature $T_{min}$, the maximum speed velocity (recorded at 1700 m) $v_{max}$. For

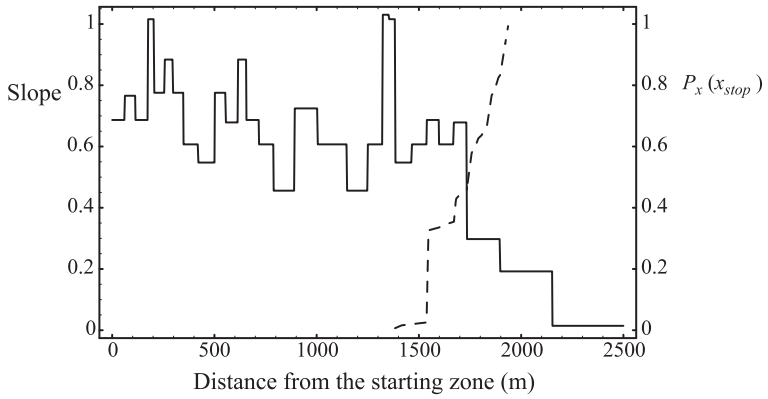


Fig. 5. Variation in the path slope as a function of the distance from the starting point (continuous line) along with the cumulative distribution function of the run-out distance for path EPA 16.

path EPA 16, the only parameter that increases the statistical test scores is the wind speed (see Table 3).

For the period for which the meteorological station has been in operation, it is possible to directly find the values of the coefficient $\mu$ for each avalanche run recorded in the database. For each event, we sought the amount of snow fallen over the previous 3 days $C_{3d}$ in the meteorological database. When this quantity was non-zero, we computed the value $\mu = Y^{-1}(x_{stop}, C_{3d}; \xi)$. Here, 24 events were recorded over the period 1980–2001 and 21 events were consecutive to snowfalls. After deducing the $\mu$ values, we computed the cumulative distribution function of $\mu$.

Table 3
Expression of the logit function for the different avalanche paths

| Number | Model | Hosmer-Lemeshow | Pearson |
|---|---|---|---|
| 12 | $-5.0450+0.0390C_{3d}$ | 0.5594 | 0.9505 |
| | $-3.9543+0.0470C_{1d}$ | 0.2402 | 0.9816 |
| 15 | $-4.9590+0.0290C_{3d}$ | 0.6301 | 0.8015 |
| | $-3.9533+0.0397C_{1d}$ | 0.6743 | 0.8003 |
| 16 | $-4.7180+0.0407C_{3d}$ | 0.6900 | 0.9894 |
| | $-3.8710+0.0420C1d+0.1025v_{max}$ | 0.7657 | 0.6896 |
| 17 | $-4.8630+0.0420C_{3d}$ | 0.8196 | 0.9810 |
| | $-3.5570+0.0475C_{3d}+0.1211T_{mean}$ | 0.8196 | 0.9810 |
| | $-3.0327+0.0437C_{3d}+0.0902T_{min}$ | 0.8806 | 0.9931 |
| | $-2.9142+0.0545C_{1d}+0.1099T_{mean}$ | 0.9054 | 0.9931 |
| | $-3.5570+0.0506C_{1d}+0.0906T_{min}$ | 0.5677 | 0.9073 |
| 27 | $-4.7270+0.0460C_{3d}$ | 0.2696 | 0.9086 |
| | $-2.7651+0.0458C_{1d}+0.0811T_{min}$ | 0.7078 | 0.9523 |
| 46 | $-4.9490+0.0280C_{3d}$ | 0.4909 | 0.8822 |
| | $-4.3274+0.0270C_{1d}+0.1128v_{max}$ | 0.5860 | 0.4640 |

Fig. 6 shows the histogram of the values obtained using the direct inversion method. The histogram does not define a regular curve but a step-shaped curve, with a first step at $\mu = 0.31$ and a second step at $\mu = 0.49$. This implies that the probability density function $p_\mu$ is not a uniformly varying function over the interval [0,1], but on the contrary varies abruptly near the two values $\mu = 0.31$ and $\mu = 0.49$. Sensibility tests have shown that the structural features of the $\mu$ distribution depend a great deal on the uncertainty on the run-out distance but, on the whole, the Voellmy-like sub-model leads systematically to a distribution of $\mu$ values around a finite set of values. We have also checked that the results are not substantially influenced by the primary choice of the $\xi$ value. This is a helpful result in the present context: it shows that we can consider $\xi$ as an independent parameter that we can adjust if we have information on the velocity reached by the avalanches at certain points of the path profile.

In parallel to the direct inversion method, we have also applied the *indirect method* presented in Section 3.3. On the same plot (Fig. 6), the resulting probability density function of the coefficient $\mu$ has been

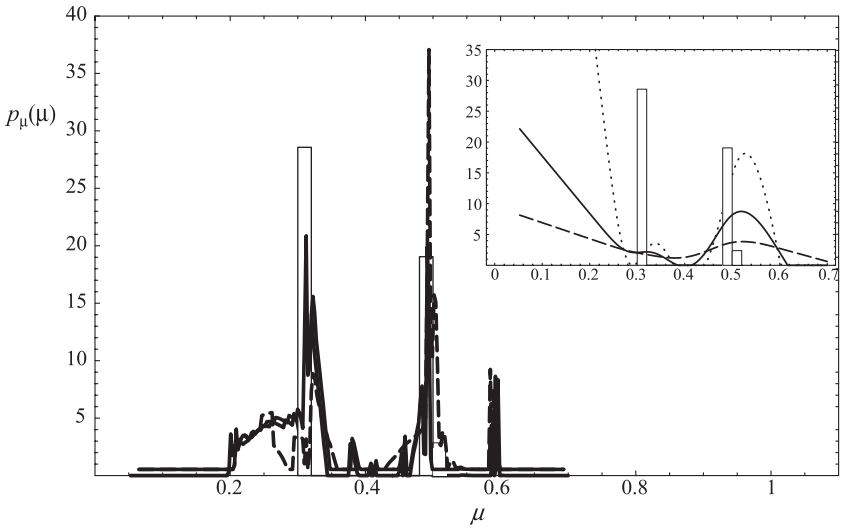


Fig. 6. Empirical probability density function of the coefficient $\mu$ for path EPA 16. The histogram (thin line) has been obtained by numerically solving the equation $x_{stop} = Y(C_{3d},\mu|\xi)$ with $\xi = 800$ m/s$^2$ and binning values into categories. The solid bold line stands for the probability density function evaluated using the indirect inversion method applied to the reduced set of run-out distances. The dashed line represents $p_\mu$ when all the events of the database are considered. In inlet we have reported the probability density function of the coefficient $\mu$ when all the events of the avalanche database are considered and when the regularization operator in the Tikhonov method is the second-order difference operator (for details, see Ancey et al., 2003).

superposed to the histogram: the long-dashed line represents the curve obtained with the full set of run-out distances (1901–2002) while the solid lined stands for the reduced set (1981–2002). Since the distribution of $\mu$ values is discrete, we have selected a regularization operator that overly limits large fluctuations (Ancey et al., 2003). The choice of another operator substantially modifies the final result; the inlet in Fig. 6 shows the sensitivity of $p_\mu(\mu)$ when the regularization operator used in the Tikhonov method is replaced by a denoising process, which tends to smooths out the peaks in the $\mu$ distribution.

An encouraging result is that the indirect inversion method provides $\mu$ values that are fairly close to those obtained by directly solving $\mu = Y^{-1}(C_{3d}|\xi)$. The main difference appearing in Fig. 6 is that the first peak at $\mu = 0.31$ is found with a wider foot. Differences between the curves obtained using the indirect inversion method on the full and reduced samples are also small; the main difference is that the wide peak around $\mu = 0.31$ observed for the reduced sample (1980–2002) is split into two peaks for the full sample (1901–2002), the first at $\mu = 0.21$ and the second at $\mu = 0.31$.

### 4.2. Summary of results obtained on other paths

The same exercise was repeated for other avalanche paths above Bessans. Table 3 summarizes the expressions of the logit function for each path. Different combinations of meteorological parameters have been studied. Here we have reported the combinations that yield the best scores (Hosmer-Lemeshow and Pearson tests).

It is seen that close avalanche paths with similar characteristics do not respond in the same way to meteorological conditions. For instance, after a snowfall of 100 cm ($C_{3d} = 100$ cm), the release probability is 11% for path EPA 15 against 34% for path EPA 16. This response difference is expected because the topographic features of the starting zone play a key role (Maggioni and Gruber, 2003). In Table 4, we have reported the $\mu$ values corresponding to peaks in the $\mu$ probability density function. The $\mu$ distribution differs from one path to another one, but note that for 6 (out of 9) paths the first peak is located at $\mu_1 = 0.16$–$0.17$, which shows a certain consistency of the results and a regional character for $\mu_1$. There are, however, three paths exhibiting a slightly different behavior. For

Table 4
$\mu$ values corresponding to the first, second, and third peak in the probability density function of $\mu$

| EPA ref. | $\mu_1$ | $\mu_2$ | $\mu_3$ |
|---|---|---|---|
| 12 | 0.24 | 0.31 | 0.34 |
| 13 | 0.17 | 0.24 | 0.28 |
| 14 | 0.17 | 0.39 | 0.43 |
| 15 | 0.17 | 0.21 | 0.26 |
| 16 | 0.20 | 0.31 | 0.36 |
| 17 | 0.16 | 0.26 | 0.41 |
| 27 | 0.16 | 0.41 | 0.47 |
| 38 | 0.18 | 0.24 | 0.47 |
| 46 | 0.16 | 0.27 | 0.32 |

Results obtained using the indirect inversion method over the full sample (1901–2002). For all avalanche paths, we took $\xi = 800$ m/s$^2$.

instance, for similar paths EPA 12 and 15, the first peak in the probability distribution function of $\mu$ is located at $\mu = 0.17$ for EPA 15 against $\mu = 0.24$ for EPA 12. Different explanations can be put forward. First of all, as explained in Section 2.1, the friction coefficient could exhibit a strong dependence on avalanche volume (Ancey, in press) and, in the meantime, could be weakly dependent on $C_{3d}$ because avalanche volume results from many other parameters such as starting-zone area and features, snow entrainment along the path, snowcover instability, etc. Second, the difference in the $\mu$ values between paths EPA 12 and 15 (despite their apparent similarities) may be a consequence of the difference in their release probability. In that case, this would mean that important processes taking place in the starting zone have been discarded in our treatment.

Other formulations (e.g. Bozhinskiy et al., 2001) have admitted that the probability density function of $\mu$ is a regularly increasing function. This assumption is not supported by the results presented here. On the contrary, the present work demonstrates that, in a SBG-like model, the coefficient $\mu$ is a discrete random variable rather than a continuous random variable.

In the present formulation of the model, there is little hope to arrive at a unique probability distribution function of the mechanical parameter $\mu$. The model can be applied to paths for which past events and meteorological conditions are known but not to paths for which no information is available. In this respect, if we remind that one of our objectives is the search of the largest applicability in engineering, the gain might be seen as low since there is not a systematic regional character in $\mu$, but the results presented in Table 4 are not too bad since 66% of the paths exhibit a very close $\mu_1$ value. Further research is needed to better understand the behavior discrepancy of some paths in line with their topographic features.

## 5. Concluding remarks

In this paper, we have explored the possibility of updating the SBG method by using it in a conceptual framework with the objective of mimicking avalanche activity in a given path over a long period. Thus, our approach lies somewhere between purely deterministic (physically based) models and statistical (black box) models and, in this respect, is not very different from the conceptual catchment models used in hydrology. Since our primary objective is to compute the run-out distance of extreme avalanches, our use of a Voellmy model appears licit; it is, however, unclear whether the method can also be applied to compute avalanche velocities and pressures with the same degree of confidence since no field data concerning these variables have been used. At this stage, our results do not support the idea according to which the friction coefficient $\mu$ is a general parameter independent of the site; the friction coefficient $\mu$ is likely to be independent of the amount of snow fallen during the days preceding the avalanche release. This can merely mean that the $C_{3d}$ variable is not the most appropriate indicator of the mobilized avalanche volume. Moreover, the coefficient $\mu$ can be approximated as a discrete random variable if, in the avalanche-dynamics model, we use the Voellmy frictional force.

Compared to other inversion methods (e.g., Bayesian approaches), the probabilistic method presented here used for fitting parameters limit the amount of a priori information on the system parameters since only one parameter remains unevaluated (the friction coefficient $\xi$). However, they do not cope with uncertainty in the run-out distance distribution. This is probably the major drawback of these two methods since the $\mu$ probability density function is affected to a varying extent by the uncertainty on $x_{stop}$. When discussing the intrinsic nature of the coefficient $\mu$, it will be necessary to determine whether the disparities in the $\mu$ distributions at different sites reflect the uncertainty of the run-out distance or a regional effect.

Compared to classic methods used in zoning, the proposed framework benefits from providing proper estimations of the run-out distance of long-return period avalanches for site where both meteorological and avalanche databases have been collected data over a sufficiently long time. The fact that the $\mu$ distribution has not a systematic regional character could be explained by one of the following explanations:

- Our framework is not refined enough (notably in the relationship between meteorological conditions and avalanche release).
- The Voellmy expression of the frictional force is too crude. In a back-analysis of 15 well-documented events in the world, we do not find any dependence of the frictional force on the square velocity (Ancey and Meunier, 2004). Moreover, if we set $\xi = 0$ (in other words, the Voellmy model is replaced by a Coulomb model in the frictional force expression), significant changes in the $\mu$ distribution are obtained (Ancey, in press).
- It is necessary to use more sophisticated element of comparison to test the similarities between two paths. As suggested by Barbolini et al. (Barbolini and Savi, 2001; Barbolini et al., 2003), paths of a same mountain range have to be categorized into different groups according to certain topographic features. Comparison between paths would make sense only if paths belong to the same group.

## Acknowledgements

This paper is a tribute to the work of André Roch, recently disappeared, and Bruno Salm, who were two of the great pioneers in the scientific study of avalanches. This study was supported by the Ministère de l'Environnement et de l'Aménagement du territoire (DPPR-MATE 2000 05 9 034 U). The authors are grateful to Eric Martin from Météo-France for providing snow data, Dominique Strazzerri for avalanche data, and Roland Burnet for the CLPA map. Urs Gruber and Massimiliano Barbolini are gratefully acknowledged for the careful reading of the paper and their helpful comments. Urs Gruber also provided a number of directions that can be followed to improve the model.

## Appendix A

We consider an avalanche with a mass $m$. We consider an idealized path profile along which the avalanche is released without velocity. The path profile can be split into two parts:

- the upper part is a straight line inclined at an angle $\theta$ with respect to the horizontal. The length is $L$;
- the lower part is a horizontal semi-infinite line.

The lag between two avalanches is assumed to be constant and corresponds to an arbitrary unit of time. The more realistic case, where the time interval between two releases is randomly distributed, can be easily addressed using hydrological methods (Coles, 2001; Reiss and Thomas, 2001).

The mass of the avalanche varies from one event to another. We denote $p_m$ the probability density function of the mass. An avalanche is assumed to experience two types of force from the plane surface:

- a Coulombic friction force with a coefficient $f$,
- a dynamic force which is a quadratic function of the velocity: $\alpha v^2$, where $\alpha$ is a constant coefficient.

The friction coefficient ranges typically from 0 to 1; here we also assumed that the value of $f$ varied from one event to another according to a probability density function $p_f$. The basic problem is the following: given the probability density functions $p_m$ and $p_f$, which are the probability density functions of variables pertaining to avalanche motion?

To that end, it is first necessary to compute the value of these variables for a given set $(m, f)$. Here we will focus on two variables of interest: the kinetic energy at a given point $A$ and the run-out distance. It can be easily shown that the kinetic energy at A is:

$$E_A = m^2 \beta (\tan\theta - f)\delta \tag{10}$$

where $\beta = g \cos\theta/(2\alpha)$ and $\delta(m) = 1 - e^{-2\alpha L/m}$ while the run-out distance is:

$$x_{\text{stop}} = -\frac{m}{\alpha}\ln(\cos\gamma) \tag{11}$$

where $\gamma = \arctan\sqrt{2\alpha\delta(m)\beta(\tan\theta - f)/(fg)}$. We are now looking for the probability density functions

associated with the kinetic energy at $A$ and the run-out distance $x_{\text{stop}}$. Referring to these quantities to as $Z$ and to $F$ as the function relating $Z$ to $f$ and $f_m$, we can express the marginal density distribution as:

$$P_Z(Z) = \int \mathrm{d}m \int \mathrm{d}f p_{f,m}(f,m) P[X \mid f,m] = \int \mathrm{d}m \int \mathrm{d}f p_{f,m} \delta(Z - F(f,m))$$

where $p_{f,m}$ is the joint density probability of $f$ and $m$ and $P[X|f,m]$ is the conditional probability of observing $Z$ given $f$ and $m$. The strategy for integrating the last equation is to use (i) the independence of parameters $f$ and $m$ and (ii) the transformation $(E_A,m)$ to $(f,m)$ to remove the Dirac term. The Jacobian of this transformation is:

$$J_E = \left| \frac{\partial E_A}{\partial f} \right| = m\beta^2\delta$$

since $\partial m/\partial f = 0$. For the run-out distance, we find:

$$J_x = \mid \partial x_{\text{stop}}/\partial f \mid = m\beta\delta\tan\theta(f^2(g - 2\beta\delta\alpha) + 2f\beta\delta\alpha\tan\theta)^{-1}$$

For the kinetic energy $E_A$, we obtain the following marginal density probability:

$$p_E(E_A) = \int J_E^{-1} p_m(m) p_f(\tan\theta - E_A/(m^2\beta\delta))\mathrm{d}m \tag{12}$$

while for the run-out distance, we obtain:

$$p_x(x_{\text{stop}}) = \int p_m(m) p_f(f(x_{\text{stop}},m)) J_x^{-1} \mathrm{d}m \tag{13}$$

A new integration leads to the cumulative distribution function, that is, the probability that the variable at hand does not exceed a given value: $P_E(E) = \Pr(E_A \le E)$. The probability that the value $E$ is exceeded is then $1 - P_E(E)$. An alternative way of expressing this is to say that, on average, the time span for observing an avalanche in which the value $E$ is exceeded is $n = (1 - P_E(E))^{-1}$.

In our context, where the interval of time corresponds to a fixed arbitrary unit of time, this number defines a characteristic time that is usually referred to as the *period of return*. Thus, here, $T_E = (1 - P_E(E))^{-1}$ is the average time required to observe an avalanche in which $E$ is exceeded. The same definition applies to other variables in the problem and thus there are as many periods of return as variables in the problem. Likewise, the order of magnitude of $T_E$ does not match that of $T_x$. Indeed, using Eqs. (10) and (11), then eliminating the friction coefficient, we deduce the variation in the run-out distance as a function of the mass and the kinetic energy at $A$:

$$x_{\text{stop}}(m, E_A) = -\frac{m}{\alpha} \ln\left( \cos \arctan \sqrt{\frac{2\alpha E_A \delta(m)\beta}{(\delta(m)m^2\beta\tan\theta - E_A)g}} \right) \tag{14}$$

From this equation it can be seen that for the distance to be a real, the kinetic energy $E_A$ cannot exceed a threshold $E_c$: $E_A \le E_c$ $(m,\theta) = \delta(m)m^2\beta\tan\theta$. For a given value of the kinetic energy and under the condition $E_0 \le E_c$, Eq. (14) defines a diffeormorphism from $\mathbb{R}_+$ to $\mathbb{R}_+$, which we denote $X$: $x_{\text{stop}} = X(m)$. A direct consequence is that the conditional probability of observing a given run-out distance (knowing that the kinetic energy at $A$ is $E_A$) is given by the expression:

$$p_a(x_{\text{stop}} \mid E_A) = \frac{p_m(X^{-1}(x_{\text{stop}} \mid E_A))}{\dot{X}(X^{-1}(x_{\text{stop}} \mid E_A))} \tag{15}$$

where $\dot{X}$ denotes the derivative of $X$ according to $m$. Thus the two density probability functions $p_E$ and $p_x$ are linked together through the following relationship: $p_x(x_{\text{stop}}) = \int_{E_A \le E_c} p_a(x_{\text{stop}} \mid E_A) p_E(E_A) dE_A$. Using the fact that $\dot{p}_E = \dot{T}_E T_E^{-2}$ (where $\dot{T}_E = \mathrm{d}T_E/\mathrm{d}E$), we finally deduce the relationship between the return periods $T_E$ and $T_x$:

$$T_x = \left( 1 - \int_{\mathbb{R}+} \mathrm{d}x_{\text{stop}} \int_{E_A \le E_c} p_a(x_{\text{stop}} \mid E_A) \dot{T}_E(E_A) \times T_E^{-2}(E_A)\mathrm{d}E_A \right)^{-1} \tag{16}$$

Thus, it is found that the return period associated with the run-out distance is linked to the return period related to kinetic energy, but in a non-trivial way due to strong non-linearity in the problem. It follows that in this example, there is little hope of finding a single variable on which a consistent return period can be computed.

What can now be done if we still want to define a return period? Different strategies can be applied to define a period of return of an avalanche. A first strategy is to directly relate this period to that corresponding to an input parameter of the problem (e.g., the mass or the friction coefficient); that is in fact the procedure followed in the SBG method. But such a strategy is not very helpful if one is interested in what happens in the lower part of the track (here on the horizontal plane). A second strategy involves considering a single variable such as kinetic energy (or impact pressure) or the run-out distance. However, a strategy of this kind would unavoidably produce paradoxical results in that under some circumstances, the avalanche can move over a very long distance with a low kinetic energy (typically for small mass and friction coefficient values) and under other conditions (typically for large mass and friction coefficient values) its motion can be characterized by a large kinetic energy value at $A$ and a short run-out distance. This problem can be avoided by considering the joint probability of observing both a run-out distance and kinetic energy (or a conditional probability of observing a run-out distance given the energy at a point): $T_{E,x}=(1-P_{E,x}(E_A,x))^{-1}$. In this case, a major problem is that there is infinity of couples $(E_A,x)$ associated with the same return period of an avalanche.

## References


Adamson, P., Metcalfe, A., Parmentier, B., 1999. Bivariate extreme value distributions: an application of the gibbs sampler to the analysis of floods. Water Resources Research 35, 2825–2832.

Ancey, C. (Ed.), 1998. Guide Neige et Avalanches: Connaissances, Pratiques, Sécurité. Edisud. Aix-en-Provence.

Ancey, C., 2001. Snow avalanches. In: Balmforth, N., Provenzale, A. (Eds.), Geomorphological Fluid Mechanics: Selected Topics in Geological and Geomorphological Fluid Mechanics. Springer, Berlin, pp. 319–338.

Ancey, C., 2004. Monte Carlo calibration of avalanches described as Coulomb fluid flows. Philosophical Transactions of the Royal Society of London A (accepted for publication).

Ancey, C., Meunier, M., 2004. Estimating bulk rheological properties of flowing snow avalanches from field data. Journal of Geophysical Research 109 (F01004).

Ancey, C., Meunier, M., Richard, D., 2003. The inverse problem for avalanche-dynamics models. Water Resources Research 39 (10.1029/2002wr001749).

Bakkehøi, S., Domaas, U., Lied, K., 1983. Calculation of snow avalanche run-out distance. Annals of Glaciology 4, 24–30.

Barbolini, M., Savi, F., 2001. Estimate of uncertainties in avalanche hazard mapping. Annals of Glaciology 32, 299–305.

Barbolini, M., Gruber, U., Keylock, C., Naaim, M., Savi, F., 2000. Application of statistical and hydraulic-continuum dense-snow avalanche models to five european sites. Cold Regions Science and Technology 31, 133–149.

Barbolini, M., Cappabianca, F., Savi, F., 2003. A new method for the estimation of avalanche distance exceeded probabilities. Surveys in Geophysics 24, 587–601.

Bartelt, P., Salm, B., Gruber, U., 1997. Modelling dense snow avalanche flow as a Criminale-Ericksen-Filby fluid without cohesion. Technical Report 717, Eidgenössisches Institut für Schnee- und Lawinenforschung (Davos).

Bartelt, P., Salm, B., Gruber, U., 1999. Calculating dense-snow avalanche runout using a Voellmy-fluid model with active/passive longitudinal straining. Journal of Glaciology 45, 242–254.

Bozhinskiy, A., Nazarov, A., Chernouss, P., 2001. Avalanches: a probabilistic approach to modelling. Annals of Glaciology 32, 255–258.

Burkard, A., Salm, B., 1992. Die Bestimmung der mittleren Anrissmächtigkeit $d_0$ zur Berechnung von Fliesslawinen. Technical Report 668, Eidgenössisches Institut für Schnee- und Lawinenforschung (Davos).

Buser, O., Frutiger, H., 1980. Observed maximum run-out distance of snow avalanches and determination of the friction coefficients $\mu$ et $\xi$. Journal of Glaciology 26, 121–130.

Chernouss, P., Fedorenko, Y., 2001. Application of statistical simulation for avalanche-risk evaluation. Annals of Glaciology 32, 182–186.

Coles, S., 2001. An Introduction to Statistical Modeling of Extreme Values. Springer, London.

Dent, J.D., Lang, T., 1980. Modelling of snow flow. Journal of Glaciology 26, 131–140.

Dent, J.D., Lang, T., 1982. Experiments on the mechanics of flowing snow. Cold Regions Science and Technology 5, 243–248.

Eglit, E., 1983. Some mathematical models of snow avalanches. In: Shahinpoor, M. (Ed.), Advances in the Mechanics and the Flow of Granular Materials. Trans. Tech. Publications, Clausthal-Zellerfeld, pp. 577–588.

Eglit, M., 1984. Theoretical approaches to avalanche dynamics. Glaciology, Soviet Avalanche Research and Avalanche Bibliography Update: 1977–1983. US Department of Agriculture Forest Service, Glaciological Data Report GD-16. World Data Center for Glaciology, pp. 63–117.

Eglit, M., 1998. Mathematical modeling of dense avalanches. In: Hestnes, E. (Ed.), 25 Years of Snow Avalanche Research, vol. 203. Norwegian Geotechnical Institute, Voss, pp. 15–18.

Fujizawa, K., Tsunaki, R., Kamishii, I., 1993. Estimating snow avalanche run-out distances from topographic data. Annals of Glaciology 18, 239–244.

Ghali, A., 1996. Méthodes statistiques pour la détermination de la distance d'arrêt des avalanches. PhD thesis, Université Joseph Fourier. Grenoble.

Gilks, W., 1996. Full conditional distributions. In: Gilks, W., Richardson, S., Spiegelhalter, D. (Eds.), Markov Chain Monte Carlo in Practice. Chapman & Hall, London, pp. 75–88.

Harbitz, C., Harbitz, A., Nadim, F., 2001. On probability analysis in snow avalanche hazard zoning. Annals of Glaciology 32, 290–298.

Hopf, J., 1998. An overview of natural hazard zoning with special reference to avalanches. In: Hestnes, E. (Ed.), 25 Years of Snow Avalanche Research, vol. 203. Norwegian Geotechnical Institute, Voss, pp. 28–35.

Hosmer, D., Lemeshow, S., 1986. Applied Logistic Regression. Wiley-Interscience, New York.

Hunt, B., 1994. Newtonian fluid mechanics treatment of debris flows and avalanches. Journal of Hydraulic Engineering 120 (12), 1350–1363.

Hutter, K., 1996. Avalanche dynamics. In: Singh, V. (Ed.), Hydrology of Disasters. Kluwer Academic Publishing, Dordrecht, pp. 317–392.

Keylock, C., Barbolini, M., 2001. Snow avalanche impact pressure-vulnerability relations for use in risk assessment. Canadian Geotechnical Journal 38, 227–238.

Keylock, C., McClung, D., Magnússon, M., 1999. Avalanche risk mapping by simulation. Journal of Glaciology 45, 303–314.

Kirsch, A., 1996. An Introduction to the Mathematical Theory of Inverse Problems. Springer, New York.

Lied, K., Bakkehøi, S., 1980. Empirical calculations of snow avalanche run-out distances based on topographic parameters. Journal of Glaciology 26, 165–177.

Maggioni, M., Gruber, U., 2003. The influence of topographic parameters on avalanche release dimension and frequency. Cold Regions Science and Technology 37, 407–419.

McClung, D., 2000. Extreme avalanche runout in space and time. Canadian Geotechnical Journal 37, 161–170.

McClung, D., 2001. Extreme avalanche runout: a comparison of empirical models. Canadian Geotechnical Journal 38, 1254–1265.

McClung, D., Lied, K., 1987. Statistical and geometrical definition of snow avalanche runout. Cold Regions Science and Technology 13, 107–119.

McClung, D., Mears, A., 1995. Dry-flowing avalanche run-up and run-out. Journal of Glaciology 41, 359–372.

McClung, D., Schaerer, P., 1993. The Avalanche Handbook. The Mountaineers, Seattle.

Mears, A., 1992. Snow-avalanche hazard analysis for land-use planning and engineering. Tech. Rep. Bull., vol. 49. Colorado Geological Survey, Denver.

Meunier, M., Ancey, C., 2004. Towards a conceptual approach to predetermining high-return-period avalanche run-out distances. Journal of Glaciology (in press).

Mougin, P., 1922. Les avalanches en Savoie, vol. IV. Ministère de l'Agriculture, Direction Générale des Eaux et Forêts, Service des Grandes Forces Hydrauliques, Paris.

Norem, H., Irgens, F., Schieldrop, B., 1986. A continuum model for calculating snow avalanche velocities. Symposium on Avalanche Formation, Movement and Effects. Davos. International Association for Hydrological Sciences, Wallingford (UK), pp. 363–379.

O'Connell, P.E., Todini, E., 1996. Modelling of rainfall, flow and mass transport in hydrological systems: an overview. Journal of Hydrology 175 (1–4), 3–16.

Press, W., Teukolsky, S., Vetterling, W., Flannery, B., 1992. Numerical Recipes in Fortran, the Art of Scientific Computing. Cambridge Univ. Press, Cambridge.

Reiss, R.-D., Thomas, M., 2001. Statistical Analysis of Extreme Values. Birkehaüser, Basel.

Robert, C., 2001. The Bayesian Choice. Springer, New York.

Salm, B., 1993. Flow, flow transition and runout distances of flowing avalanches. Annals of Glaciology 18, 221–226.

Salm, B., Burkard, A., Gubler, H. 1990. Berechnung von Fliesslawinen, eine Anleitung für Praktiker mit Neispielen. Tech. Rep. No 47, Eidgenössisches Institut für Schnee- und Lawinenforschung (Davos).

Savage, S., 1989. Flow of granular materials. In: Germain, P., Piau, J.-M., Caillerie, D. (Eds.), Theoretical and Applied Mechanics. Elsevier, Amsterdam, pp. 241–266.

Savage, S., Hutter, K., 1989. The motion of a finite mass of granular material down a rough incline. Journal of Fluid Mechanics 199, 177–215.

Schaerer, P., 1974. Friction coefficients and speed of flowing avalanches. Symposium Mécanique de la Neige, vol. 114. IAHS, Grindelwald, pp. 425–432.

Tai, Y.-C., Hutter, K., Gray, J., 2001. Dense granular avalanches: mathematical description and experimental validation. In: Balmforth, N., Provenzale, A. (Eds.), Geomorphological Fluid MechanicsLecture Notes in Physics, vol. 582. Springer, Berlin, pp. 339–366.